Forward Directed Smith-Purcell Radiation from Relativistic Electrons

K. J. Woods and J. E. Walsh
Department of Physics and Astronomy, Dartmouth College, Hanover, New Hampshire 03755

R. E. Stoner*
Massachusetts Institute of Technology and Research Laboratory of Electronics, Cambridge, Massachusetts 02139

H. G. Kirk and R. C. Fernow
Department of Physics, Brookhaven National Laboratory, Upton, New York 11973
(Received 12 December 1994)

The requirements for the generation of forward directed Smith-Purcell emission from relativistic electrons are introduced, and the first experimental evidence of this phenomenon is presented. The experiments were conducted with a 2.8 MeV/c electron beam interacting with a 1 cm period grating. Radiation emitted in two bands with wavelengths ranging from 600 to 650 μm and 1.2 to 1.7 mm were measured. Grating period to wavelength ratios were as high as 16. The measured intensities are higher than that predicted by incoherent emission.

PACS numbers: 41.60.–m, 41.75.Ht, 42.79.Dj

The characteristic signature of radiation produced by energetic electrons is a peaking of the emission spectrum along the direction of the electron momentum. Thus it is to be expected on general grounds that Smith-Purcell radiation produced by relativistic electrons will exhibit this structure as well. In this limit the source will have a very small effective area, and a narrow angular range will contain a large frequency range, both of which are very desirable properties for potential spectroscopic applications. The first experimental evidence of forward emission from relativistic electrons will be presented in this Letter.

In their report on radiation produced by electrons skimming over a diffraction grating, Smith and Purcell [1] introduced the expression

$$\lambda = \frac{l}{|n|}[1/\beta - \cos(\theta)], \tag{1}$$

which relates wavelength λ, grating period l, the relativistic velocity of the electron β, the emission angle θ, and the diffraction order $|n|$. The emission angle is measured relative to the axis established by the electron's momentum. Equation (1) may be deduced from a Huygens construction, and the expression is valid in either the nonrelativistic or relativistic limit. When $\beta \rightarrow 1$, forward emission at $\theta \rightarrow 1/\gamma$ (γ being the relativistic factor $1/\sqrt{1-\beta^2}$) will result in wavelengths that are much shorter than the grating period. In order to maintain good coupling between the electron beam and the grating for emission in the forward direction, additional constraints must also be satisfied.

The angular distribution of the power radiated into the nth order from electrons moving over a grating is given by an expression of the general form

$$\frac{dP_n}{d\Omega} = \frac{eIn^2L\beta^3}{2l^2\epsilon_0}\frac{\sin^2(\theta)\cos^2(\phi)}{[1-\beta\cos(\theta)]^3}[1 + N_e\mathcal{F}(\alpha)] \times \exp[-\kappa(\theta,\phi)x_0]|R_n(\theta,\phi)|^2 \ (\mathrm{W/sr}), \tag{2}$$

where L is the total grating length, I is the beam current, e is the charge of an electron, N_e is the number of electrons per bunch, ϵ_0 is the permittivity of free space, α is related to the electron bunch length τ by $\alpha = 2\pi|n|c\tau/l[1-\beta\cos(\theta)]$, and x_0 is the beam height measured from the highest point on the grating surface. An expression similar to Eq. (2) was first published by Toraldo di Francia [2], and many general considerations relating to the intensity of the emission were addressed originally by Smith [3]. Equation (2) can be derived also from an elementary model of the emission mechanism [4].

The coordinate system and emission angles θ and ϕ are illustrated in Fig. 1. The wavelength depends only on the polar angle θ, and it should be noted that the solid angle $d\Omega$ and signal bandwidth $d\omega$ are related through Eq. (1). Equation (2) is derived using a delta function beam located at $x = x_0$, $y = 0$. This is a good approximation for an extended beam if the mean beam height satisfies the condition $x_0 < \beta\gamma\lambda/4\pi$. If this condition is not satisfied, an integral over the beam distribution must be substituted for the exponential term.

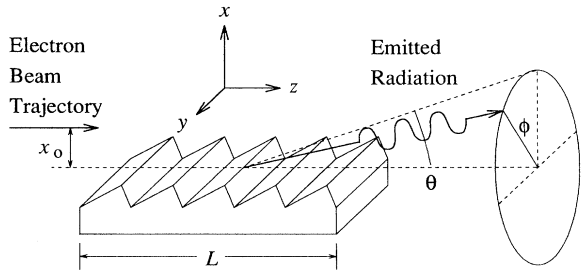

FIG. 1. Diagram showing the coordinate system and angles which define the direction of the emitted radiation. The beam axis is in the z direction, and x is normal to the grating plane. θ is the polar angle, and ϕ is the azimuthal angle.

 0031-9007/95/74(19)/3808(4)$06.00

The function $\mathcal{F}(\alpha)$ is introduced in order to account for possible intensity enhancement due to temporal coherence of the electron bunch. This concept was first discussed during the early development of synchrotrons, where it was suggested that it could be a possible mechanism for substantial energy loss [5].

Exclusive of the $|R_n(\theta,\phi)|^2$ term, the angular distribution of the radiation is determined by the two factors $\sin^2(\theta)\cos^2(\phi)/[1-\beta\cos(\theta)]^3$ and $\exp[-\kappa(\theta,\phi)x_0]$. When $\theta \to 1/\gamma$ the dependence of the first of these terms scales as γ^4 near its peak, and the peak narrows in proportion to $1/\gamma^3$. For relativistic electrons the peak can be sufficiently narrow so $|R_n(\theta,\phi)|^2$ is approximately constant and contributes little to the angular variation in this range. The exponential factor $\exp[-\kappa x_0]$ is a consequence of the fact that the electron beam couples with space harmonic fields on the grating which have a phase velocity less than the speed of light. The evanescent scale is [4]

$$\kappa(\theta,\phi) = \frac{2\omega}{c\beta\gamma}\sqrt{1+[\beta\gamma\sin(\theta)\sin(\phi)]^2}, \tag{3a}$$

or, invoking Eq. (1),

$$\kappa_n = \frac{4\pi|n|\sqrt{1+[\beta\gamma\sin(\theta)\sin(\phi)]^2}}{\gamma[1-\beta\cos(\theta)]l}. \tag{3b}$$

It follows from Eq. (3b) that in the limit $\theta \to 1/\gamma$, $\beta \to 1$, the scaling $4\pi x_0/l \simeq 1/\gamma$ must be maintained in order to prevent the exponential factor from cutting off the emission in the forward direction. Thus the possibly surprising conclusion is reached that l must become quite large in order to maintain good coupling for small emission angles. The emitted wavelength in this limit scales as $\lambda \simeq l/\gamma^2$.

The only factor not yet discussed is $|R_n(\theta,\phi)|^2$ which, in essence, is a measure of grating efficiency. The concept was first introduced for Smith-Purcell radiation by Toraldo di Francia [2], and later van den Berg [6] devised a method for calculating $|R_n(\theta,\phi)|^2$. The van den Berg approach is straightforward but numerically intensive when wavelengths are much shorter than the grating period [7]. Since in this limit the grating period is long in comparison with the emitted wavelength, the grating falls into a class known generally as an echelle [8].

The experimental investigations were conducted on the Accelerator Test Facility (ATF) low-energy beam line at Brookhaven National Laboratory [9]. The beam line consists of a $1\frac{1}{2}$ cell rf photoinjector, profile monitors, momentum slits, a dipole magnet, and focusing quadrupole magnets, as well as horizontal and vertical steering magnets. The momentum was tuned to 2.8 MeV/c ($\gamma = 5.6$). The π-mode S-band injector contains a photocathode which was operated in an explosive electron emission mode. Explosive electron emission results from irradiating the cathode with a reduced spot size of a frequency-quadrupled Nd:YAG pulse so that higher laser power densities on the cathode are achieved [10]. The macropulses are typically 20 ns long (57 rf buckets) and contain 2 nC of charge. The repetition rate was 3 Hz. The micropulses are 20 ps long and separated by 350 ps. The measured emittances are on the order of 4π mm mrad and peak currents are typically 1–2 A.

The optical collection system is one used previously [11]. As shown in Fig. 2, the Smith-Purcell emission from the grating is reflected off a rotatable plane mirror onto an off-axis parabodial mirror (OAPM). Adjusting the plane mirror angle allows the selection of the desired observation angle and therefore the wavelength of the Smith-Purcell radiation. The OAPM focuses the radiation into a light pipe which transports the signal to an optical table. The light pipe was not evacuated.

A beamflag consisting of a phosphor painted aluminum surface was mounted at the front of the grating assembly to allow viewing of the beam profile by a video camera. The video signal was analyzed by a SPIRICON imaging system which allowed a measurement of the beam width, height, and charge distribution. The beam was approximately Gaussian in both directions with a width of 1.2 cm and a thickness normal to the grating of 0.75 mm. The grating height was adjusted so a small fraction of the beam was intercepted by the grating.

The optical collection system was originally designed for viewing emission angles larger than 30°, but for this experiment it was modified to allow collection at smaller angles. The collection system's angular width was approximately 10°, and the emission spectrum was centered about the nominal collection angle.

The spectral content of the radiation was analyzed with a Czerny-Turner monochromator and detected with a liquid helium cooled InSb bolometer. The detector and amplifier system responsivity was calibrated at 623 μm with a 5000 K mercury arc lamp and the monochromator. The measured responsivity was 862 V/W for radiation pulse lengths much longer than the response time of the crystal. The responsivity was also measured with an

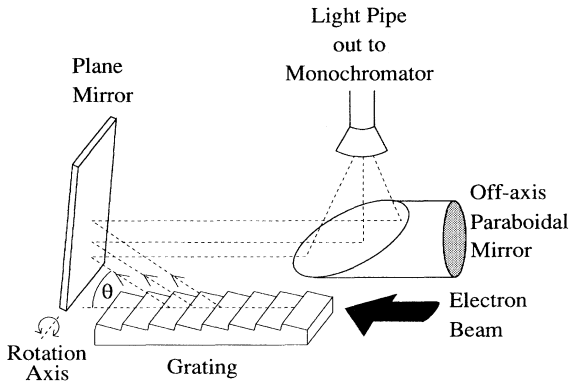

FIG. 2. Geometry of the Smith-Purcell collection system. The dashed lines indicate the path of the emitted radiation and θ defines the emission angle.

optically pumped far-infrared laser at a wavelength of 432 μm, and when the responsivity was corrected for the wavelength dependence of the responsivity the value agreed well with the arc lamp calibration. Since the radiation signal (20 ns) is only a fraction of the response time of the detector crystal (180 ns), the detector serves as an energy detector rather than a power meter. Integration of the detector signal gives the energy deposited on the crystal. However, since the bolometer signal has a very sharp rise and falls off exponentially as the electrons relax to the lattice temperature, the area under the curve is simply the signal amplitude times the relaxation time. This allows the computation of an effective responsivity of the detector which is

$$R_{\text{eff}} = 862 \text{ V/W} \times \frac{20 \text{ ns}}{180 \text{ ns}} = 95.8 \text{ V/W}.$$

The signals were averaged over 16 shots on a Tektronix 2431L digital oscilloscope.

An aluminum grating 1.69 cm wide and 17 cm long with a period of 1.0 cm and a blaze angle of 5° was used to investigate forward emission. It was oriented (Fig. 2) such that the electron footprint moves up the shallow slope of the grating. In addition to the grating just described, wavelength measurements were conducted with 30° blaze gratings which had periods of 1, 2, and 4 mm and 20° blaze gratings with periods of 2 and 4 mm. Measured emission angles ranged from 18° to 140°. The measured wavelengths, shown in Fig. 3, are in excellent agreement with the predictions of Eq. (1).

Forward emission observations were made at nominal collection angles of 18° and 30°. The 30° orientation was chosen because that was the smallest angle for which good collection efficiency could be expected [12]. The 18° setting was examined because it is near the peak of the power spectrum as given by Eq. (2) in the limit $\mathcal{F}(\alpha) = 0$. The spectral content of the two settings are shown in Figs. 4 and 5. The detector signal was normalized to the charge measured at the Faraday cup to reduce the small effect of shot-to-shot variations of about 15%. A linear relationship between the signal and charge was assumed for this normalization.

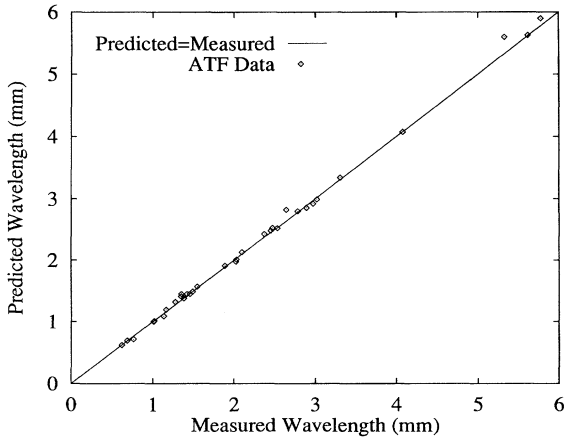

FIG. 3. Plot of predicted vs experimental wavelengths.

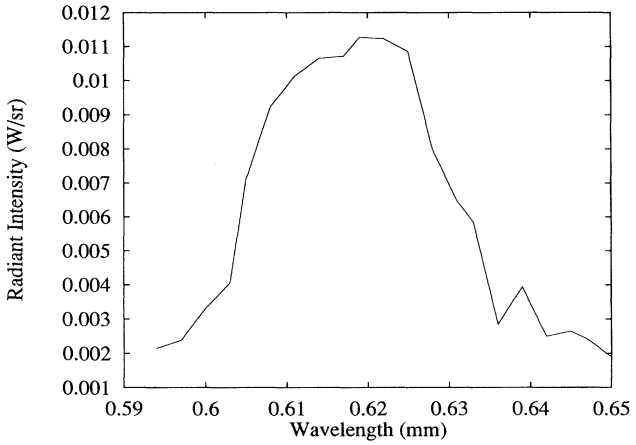

FIG. 4 Plot of the experimentally measured radiant intensity at the nominal 18° collection angle. The experimental measurements have been scaled by a factor of 2 to account for the intensity from the entire grating.

In other experiments [13–15] where the long pulse nature of the electron beam makes the limit $\mathcal{F}(\alpha) \to 0$ appropriate, the results indicate that the predicted and measured powers are comparable. Thus Eq. (2) is a reliable predictor of the spontaneous emission from a group of uncorrelated electrons. For our experiment the measured power was significantly higher than the prediction of Eq. (2) for $\mathcal{F}(\alpha) = 0$. The macropulse average powers measured at the detector were 62.6 μW for a wavelength of 0.623 mm. For the 18° setting only the back half of the grating, or about eight periods, was collected by the collection system so the power from the entire grating would be a factor of 2 higher. At 30° the measured power was 70.7 μW at a wavelength of 1.32 mm.

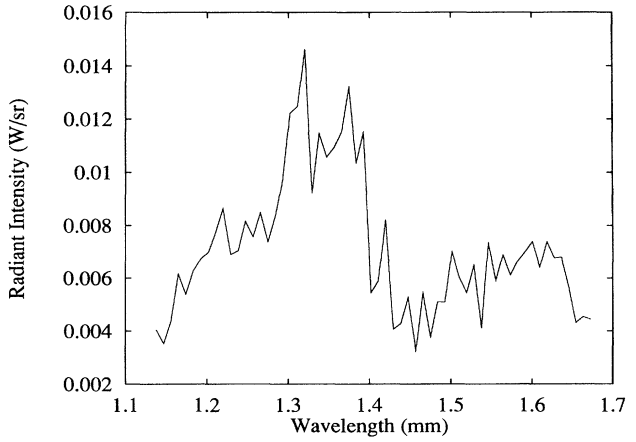

FIG. 5. Plot of the experimentally measured radiant intensity at the nominal 30° collection angle.

In order to compare the measured power with that predicted by Eq. (2) a calculation of $|R_{-1}(\theta,0)|^2$ is needed. Following the integral method of van den Berg, a Fourier series method code was developed to perform the necessary calculation. For a wavelength 16 times smaller than the grating period there are 32 radiating harmonics. This implies that the Fourier series should contain about 64 harmonics with each harmonic being the sum of 128 terms [16]. The calculation of $|R_{-1}(\theta,0)|^2$ including 101 harmonics and 202 terms gives $|R_{-1}(\theta,0)|^2 = 0.135$ at 17.4°, corresponding to a wavelength of 0.623 mm at an energy of 2.3 MeV. At an angle of 27.8°, corresponding to a wavelength of 1.32 mm, $|R_{-1}(\theta,0)|^2 = 0.210$. van den Berg also derived an equation which serves as a conservation of energy check between the radiating orders and the incident evanescent wave which was satisfied to less than 5% for the calculation. The value of $|R_{-1}(\theta,0)|^2$ varies between 0.125 and 0.175 over the range in Fig. 4 and between 0.20 and 0.33 over the range in Fig. 5.

In the limit $\mathcal{F}(\alpha) = 0$ (no coherence) the emission levels predicted by Eq. (2) for the experimental parameters ($I_{\text{avg}} = 0.108$ A, $L = 17$ cm, $l = 1.0$ cm, $\beta = 0.9838$, $x_0 = 0.3$ mm) is 27.6 μW/sr for 0.623 mm ($\theta = 17.4°$) and 19.6 μW/sr for 1.32 mm ($\theta = 27.8°$). The detected solid angles of 0.012 sr at 17.4° and 0.0054 sr at 27.8° are determined by the bandwidth passed by the monochromator, which through the Smith-Purcell relationship determines the range of the polar angle, and the plane mirror width which determines the azimuthal angular range. These values for the solid angles lead to emission power levels of 0.33 μW at 0.623 mm and 0.11 μW at 1.32 mm. The measured power levels exceed the predictions by a factor of almost 200 at 0.623 mm and by almost 700 at 1.32 mm. Including losses from the collection system and spectrometer would make these ratios even higher. The leading candidate for explaining why the observed powers exceed predictions based on single particle theory is temporal coherence of the emission process. If the electron bunch was Gaussian, coherent enhancement would not be expected at wavelengths shorter than the electron bunch. But if the bunch had an alternative profile such as rectangular, the coherent enhancement would have a higher harmonic content which would extend the coherent enhancement to shorter wavelengths and produce peaks in the emission spectrum similar in width to those measured. Coherent emission would also be consistent with the observation that the ratio of measured to predicted is higher at longer wavelengths. Estimating the collection and detection efficiency to be 5% would imply a coherent enhancement of $\sim 10^4$. This is significantly less than the $\sim 10^8$ electrons in the microbunches, suggesting only partial coherence.

It is interesting to compare the Smith-Purcell emission to a conventional source of far-infrared radiation. A blackbody at a temperature of 5000 K and the same effective area as the grating emits only 0.345 μW in the bandwidth defined in Fig. 4. The Smith-Purcell macropulse signal is more than 2 orders of magnitude larger than the blackbody. This ratio is similar to that achieved by synchrotron radiation in the far-infrared [17], which in recent years has become a very important tool for Fourier transform spectroscopy research in this spectral regime.

The authors would like to thank the staff at the ATF and in particular X. Wang whose efforts made this experiment possible. We also thank M. F. Kimmitt for his assistance in calibration of the detector and for use of his grating monochromator. We gratefully acknowledge support from U.S. Army Research Office Grant No. DAAL03-91-G-0189 and Department of Energy Contract No. DE-AC02-76-CH00016.

*Present address: Smithsonian Astrophysical Observatory, Cambridge, Massachusetts 02140.

[1] S. J. Smith and E. M. Purcell, Phys. Rev. **92**, 1069 (1953).
[2] G. Toraldo di Francia, Nuovo Cimento **16**, 61 (1960).
[3] S. J. Smith, Ph.D. thesis, Harvard University, 1953.
[4] J. Walsh, K. Woods, and S. Yeager, Nucl. Instrum. Methods Phys. Res., Sect. A **341**, 277 (1994).
[5] J. S. Nodvick and D. S. Saxon, Phys. Rev. **96**, 180 (1954).
[6] P. M. van den Berg, J. Opt. Soc. Am. **63**, 1588 (1973).
[7] O. Haeberlé, P. Rullhusen, J.-M. Salomé, and N. Maene, Phys. Rev. E **49**, 3340 (1994).
[8] G. R. Harrison, J. Opt. Soc. Am. **39**, 522 (1949).
[9] K. Batchelor *et al.,* Nucl. Instrum. Methods Phys. Res., Sect. A **318**, 372 (1992).
[10] X. J. Wang *et al.,* J. Appl. Phys. **72**, 888 (1992).
[11] G. Doucas, J. H. Mulvey, M. Omori, J. Walsh, and M. F. Kimmitt, Phys. Rev. Lett. **69**, 1761 (1992).
[12] At emission angles smaller than 30° some of the emitted radiation passes below the plane mirror.
[13] G. Doucas, J. H. Mulvey, M. Omori, J. Walsh, and M. F. Kimmitt, Nucl. Instrum. Methods Phys. Res., Sect. A **331**, 609 (1993).
[14] A. Gover, P. Dvorkis, and U. Elisha, J. Opt. Soc. Am. B **1**, 723 (1984).
[15] M. Goldstein, Ph.D. thesis, Dartmouth College, 1994.
[16] R. Petit, *Electromagnetic Theory of Gratings* (Springer-Verlag, Germany, 1980), p. 25.
[17] G. P. Williams, Rev. Sci. Instrum. **63**, 1535 (1992).